



Analysis of Shoulder Driven Zone Formation in Friction Stir Welding Using Advanced Scroll Tool

David Yan  and Logan Vahlstrom

Submitted: 8 January 2021 / Revised: 17 May 2021 / Accepted: 16 June 2021 / Published online: 6 July 2021

The main objective of this work is to reveal the forming mechanism of the shoulder driven zone during scroll tool friction stir welding (FSW). Scroll tools are widely used in FSW as they offer extra advantages of eliminating the tilted tool axis that is usually employed during the process. Therefore, it is vital to understand the forming mechanism of the shoulder zone when using an advanced scroll tool, which is important for optimizing welding parameters, analyzing welding defects, and controlling microstructure and properties of welds. In this present study, a series of FSW of thick section 6061 Al-T6 and Cu-AstmB370 (Cu foil as tracer) trials was conducted. A novel marker-insert technique by placing the Cu foil outside the welding path was employed, and the zonal flow patterns were characterized via OM, SEM and EDS. For the first time, the material flow behavior and actual flow patterns in the shoulder zone were detected by observing the distribution of Cu foil fragments in the weld zone. It was found that the thickness of shoulder zone varies along the weld transverse cross section with the thicker portion on the advancing side than the retreating side. The flow pattern of the shoulder driven zone reveals that a simple layer-to-layer banded structure appeared in the bottom portion of shoulder driven zone, whereas a featureless flow pattern showed in the top portion of the shoulder zone. Accordingly, the forming mechanism of shoulder driven zone was revealed based on the identified flow patterns.

1. Introduction

Since friction stir welding (FSW) was introduced by The Welding Institute (TWI), UK in 1991, understanding of material flow in FSW has attracted significant interest. As a thorough understanding of the material flow behavior helps optimize the welding parameters for controlling microstructure and properties of welds (Ref 1). During FSW, material primarily moves in two zones: shoulder driven zone (i.e., shoulder flow zone or shoulder zone) and pin driven zone. The movement of material in these two zones is mostly circumferential around the FS tool pin and beneath the FS tool shoulder (Ref 2). Indeed, material flow results in the formation of different weld zones or weld defects (quality of the weld), and special marker materials were used to trace and mark the material flow path since the process could not be observed directly (Ref 3-5).

Recently, researchers (Ref 6, 7) have employed different techniques and models in attempting to establish the material flow movement during FSW, as well as flow patterns for revealing the mechanism of weld zone formation. The forming mechanism of the different weld zones using conventional shoulder tool (i.e., tilted-tool) has been well addressed by Mishra and Ma (Ref 8) in their review of friction stir welding and processing. It is commonly known that a featureless flow pattern appears within the shoulder driven zone and a serial near-semicircular banded structure or so-called onion-rings structure can be observed in the nugget zone sectioned parallel to the welding direction (Ref 8). Kumar and Kailas (Ref 9) studied the material flow during tilted-tool FSW, and found that

the featureless flow pattern in the shoulder driven zone is resulted from a bulk flow mode of the plasticized material flows into the shoulder zone. Chen et al. (Ref 10) investigated the effect of pin thread on the material flow behavior in tilted-tool FSW of AA7A52 plates using 0.1 mm thick Cu foil as tracer, and reported that a many-circle flow pattern around the pin can be observed. Huang et al. (Ref 11) visualized the material flow by copper foil markers during tilted-tool FSW of 6082 Al alloy, and concluded that shoulder driven flow drives materials from the retreating side to the advancing side and causes the bulge structure to have a thicker portion in the retreating side than in the advancing side. While pin-driven flow mainly extrudes material to the retreating side. Chen et al. (Ref 12) studied nugget zone (i.e., pin driven zone) formation during tilted-tool FSW 5083 Al alloy and reported that the nugget zone is formed by a shear layer material which detaches in the trailing-retreating location of tilted tool pin, one layer in each revolution. Layer-to-layer detachments lead to a serial near-semicircular banded structure appearing in the nugget zone of the weld.

Study of weld zone formation using advanced scroll tool (i.e., non-tilted tool) has been an area of interest in recent times. According to Rai et al. (Ref 13), the scroll tool offers an additional advantage of allowing elimination of the tilted tool axis that is usually applied in conventional shoulder tool FSW. Donatus et al. (Ref 14) summarized the existing material flow theories reported in the literature, and concluded that the material flow during FSW is complicated and far from being fully understood and established. They studied material flow behavior during scroll tool FSW 8 mm thick AA5083 and AA6082-Al plates, and found that the weld zone material is pushed by the tool and flows more from the advancing side into the retreating side without mixing (Ref 14).

Although a number of weld zone flow patterns have been presented by Donatus et al. (Ref 14) and Tozaki et al. (Ref 15)

David Yan and Logan Vahlstrom, Department of Aviation and Technology, San José State University, One Washington Square, San Jose, CA 95192. Contact e-mail: david.yan@sjsu.edu.

during scroll tool FSW, the exact flow pattern in the shoulder driven zone has not been fully characterized. The forming mechanism of the shoulder zone during scroll tool FSW is not yet clearly understood as well. Indeed, the findings of Huang et al. (Ref 11) and Donatus et al. (Ref 14) on the material flow behavior in weld zone contradicted each other. Moreover, the tracer technique using markers has not been employed during scroll tool FSW to establish the actual material flow patterns in the shoulder zone.

In this study, experimental studies were performed on FSW of 20 mm thick 6061Al-T6 plates with 0.127 mm thick Cu-Astm B370 foil as marker material to trace material flow during FSW. For the first time, the Cu foil was originally placed outside the welding path to track the shoulder zone material flow movement. The produced welds were sectioned, mounted and polished with standard metallographic practice, and etched using Keller's reagent. The etched samples were characterized by optical microscopy (OM) and scanning electron microscopy (SEM) equipped with energy-dispersive X-Ray spectroscopy (EDS) to identify the shoulder driven zone and zonal flow pattern. The distribution of Cu foil fragments was analyzed to study the material flow behavior, particularly how the weld zone material flows during the depositing process in the trailing side of the rotating tool shoulder. The forming mechanism of the shoulder zone was revealed based on the identified flow pattern.

2. Experimental Procedures

A milling machine was employed to perform FSW with conventional rigid clamping and steel backing. A non-tilted, one scroll flat shoulder and tapered pin tool was made of H13 tool steel and utilized during FSW. The tool shoulder diameter was 30 mm, and a scroll groove with 3.5 mm pitch, 1.5 mm width and 1.3 mm depth was cut into the shoulder face, which enabled the tool to perform FSW at 0° tool tilt angle. The tool pin had a large core volume with an 18.8 mm length, 5.0 mm tip diameter and 8° cone angle. Commercial 20 mm thick 6061Al-T6 (composition in weight %: Mg 1.17, Si 0.57, Cu 0.26, Fe 0.45, Cr 0.22, Al remaining) plates were used as workpiece. Figure 1 illustrates the FSW process and indicates the locations of shoulder flow zone (solid line), nugget zone

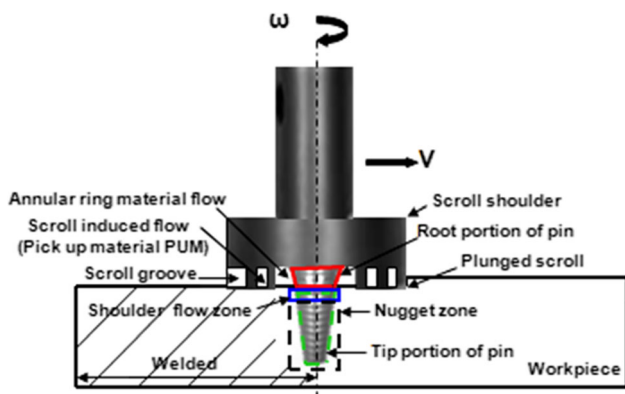


Fig. 1 Schematic illustration of the scroll tool FSW process, showing the locations of shoulder flow zone and nugget zone and components of the tool

(dashed line), pick-up material and annular ring material, and components of the scroll tool.

A 0.127 mm thick Cu-Astm B370 foil (99.99% purity) was used as a marker to trace material flow during FSW. A 'marker-insert' specimen was constructed such that a piece of copper foil was inserted along the advancing side of the workpiece with a 13 mm offsetting from the welding center line and aligned with the top surface of the workpiece. Figure 2 illustrates the location and direction of potential marker movement.

A series of FSW experiments (including tracer technique using Cu foil markers) was conducted by perpendicularly plunging the scroll shoulder into the workpiece to a depth of 0.4, 0.5 and 0.6 mm, respectively. While the tool was constantly rotating at 250 rpm, and subsequently feeding along the welding center line at a constant speed of 40 mm/min for a 200 mm length.

The 'marker' movement during FSW was hypothesised such that firstly, after plunging the rotating scroll shoulder into the marker-insert workpiece to the designated depth, the edge of the scroll beneath the tool shoulder could cut, soften and mix the Cu foil with Al workpiece to form the pick-up material. Secondly, when the tool was traveling forward simultaneously, the new Cu foil could be sheared into small Cu fragments one per revolution by the rotating scroll edge, then the Cu fragments could be mixed with the softened Al workpiece to form the new pick-up material. Lastly, the pick-up material could follow the scroll groove and be driven into the center spacing of the scroll groove (i.e., spacing of annular ring material flow shown in Fig. 1), then the annular ring material including small Cu fragments could be driven downward by the rotating threaded tool pin and distributed within the weld zone. If any small Cu fragments are found in the weld zone, the zone mixed with the Cu fragments is in fact the shoulder driven zone. Indeed, the Cu foil was originally placed outside the welding path and stir zone in this present study, which was different to all reviewed marker-insert literature including the work of Huang et al. (Ref 11), of which the Cu foil was placed within the stir zone along the welding center line.

After the welds were made, the specimens were sectioned in the transverse and longitudinal directions (all through the welding center line unless indicated) and used for the metallographic examination. The sectioned samples were mounted and polished with standard metallographic practice followed with 0.3 μm Alumina-water slurry for final polishing, and etched using Keller's reagent (1 ml HF, 1.5 ml HCl and 2.5 ml HNO₃ in 95 ml H₂O). Then the etched samples were characterized by OM and SEM equipped with EDS to identify the actual shoulder flow zone and zonal flow pattern. The distribution of Cu foil fragments in the weld zone was revealed through the longitudinal cross section of the weld made at a 0.5 mm depth of tool shoulder penetration.

3. Results and Discussion

3.1 Shoulder Zone Configurations

Figure 3(a), (b) and (c) shows a post-weld profile, micrographs of the transverse and longitudinal cross section of the weld, respectively, obtained at a 0.4 mm depth of tool shoulder penetration with tool rotating (ω) while traveling (V) constantly

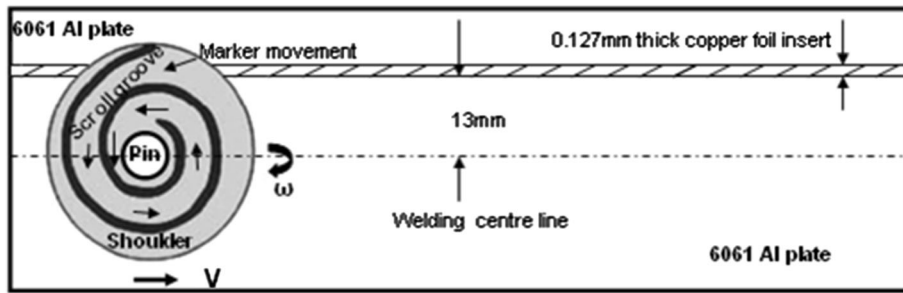


Fig. 2 Schematic illustrations of the 'marker-insert' configuration and direction of marker movement, viewed on x-y plane

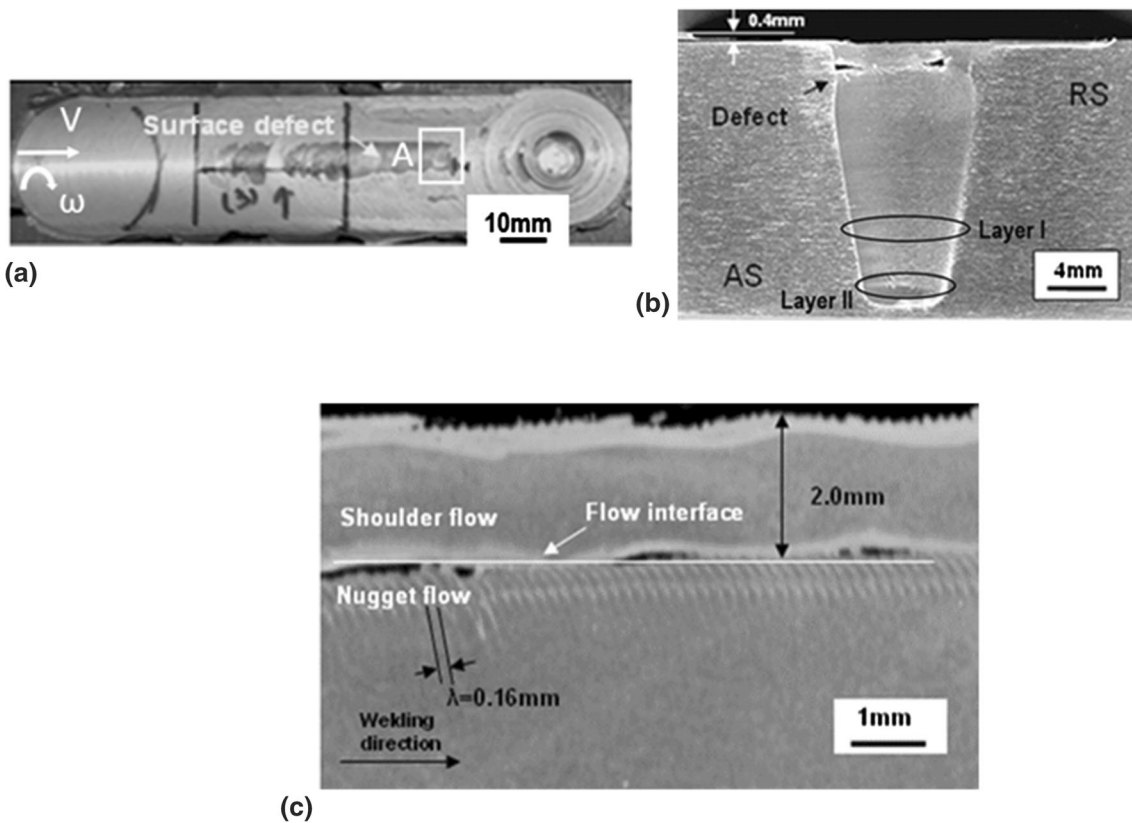


Fig. 3 Optical macrographs of weld obtained at 0.4 mm depth of shoulder plunging with tool rotating while traveling at constant speeds 250 rpm and 40 mm/min, (a) post-weld profile showing surface defect in the marked area 'A', (b) weld transverse cross section showing internal defect (voids) on both AS and RS, and (c) top portion of the weld longitudinal cross section indicating a potential flow interface to distinguish between shoulder flow zone (thickness= 2.0 mm) and nugget flow zone, and showing a banded structure of nugget zone flow pattern (band spacing $\lambda = 0.16$ mm)

at 250 rpm and 40 mm/min. It can be observed that the surface defect appeared on the post-weld profile and two internal defects (i.e., voids) occurred in the weld transverse cross section on both advancing side (AS) and retreating side (RS). A simple banded structure presented within the weld longitudinal cross section with a band spacing: $\lambda = V \div \omega = 40 \text{ mm/min} \div 250 \text{ rpm} = 0.16 \text{ mm}$, according to Krishnan's findings (Ref 16). Internal voids also occurred in the weld longitudinal cross section, which can be used as a flow interface to distinguish between the shoulder flow and nugget flow, and the measured shoulder zone thickness was 2.0 mm. It was clear from

Fig. 3(b) that a special corn-shaped pattern can be found in the weld zone presenting with several stacked layers, e.g., layer I and II from top to bottom, instead of showing a conventional onion-rings structure. This weld zone pattern is similar to the four stacked layers reported by Huang et al. (Ref 11), for which they attributed the zonal pattern to the features of the tool pin. It appears that the corn-shaped with stacked layers pattern shown in Fig. 3(b) corresponds well to the tapered pin tool (Fig. 1) used in this present study. And so, the stacked layer pattern in the weld zone is likely a result of material deposition behind the rotating threaded tool pin, as the presence of threads in the FS

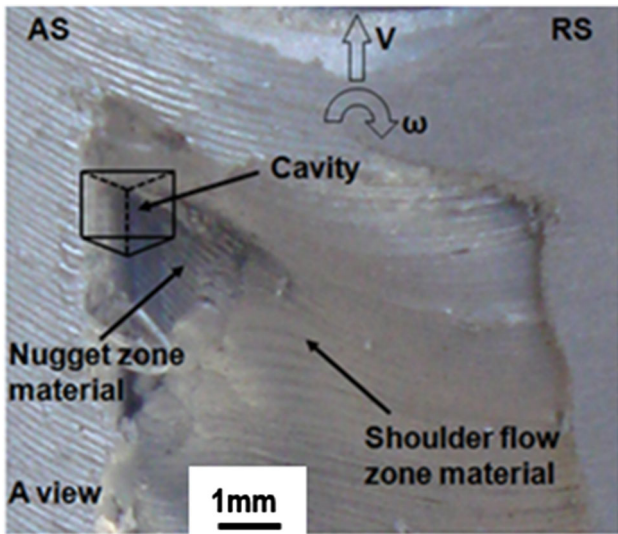


Fig. 4 Optical macrograph (enlarged view) of the area 'A' marked in Fig. 3(a), showing the weld zone configuration with shoulder flow zone (illustrated as a weld cavity) located at the top portion of the weld, while the nugget zone positioned beneath the shoulder zone, and a thicker shoulder zone on the advancing side and vice versa

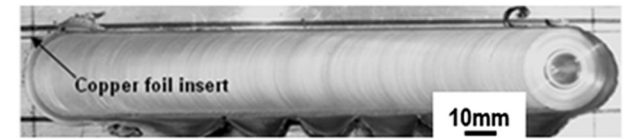
tool pin can induce additional material movement in the vertical direction, based on the findings of Gotawala and Shrivastava (Ref 2).

Figure 4 presents an enlarged view of the area 'A' marked in Fig. 3(a) to depict the weld zone configurations. It can be seen that the shoulder flow zone, illustrated as a weld cavity, existed along the advancing side of the weld and had a deeper depth toward the advancing side when measured from the post-weld surface. This finding is in contrast to the conceptual model of shoulder zone developed by Huang et al. (Ref 11), in which they constructed a thicker portion of the shoulder driven flow on the retreating side. In fact, the thickness of the shoulder zone varies across the entire weld transverse cross section with the thicker portion on the advancing side based on the obtained weld zone configuration shown in Fig. 4.

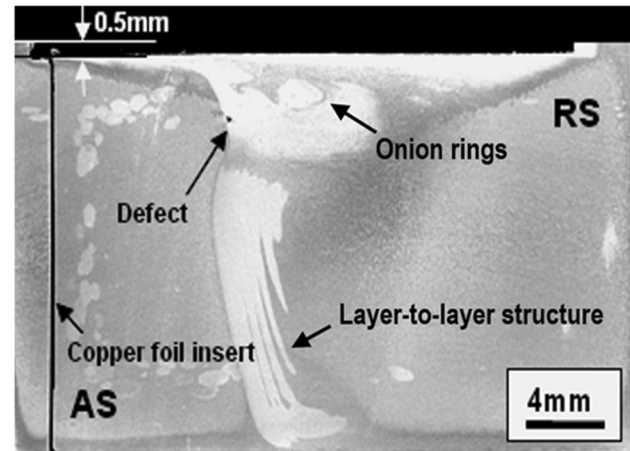
This weld cavity offers a positioning reference to the nugget zone which can be located beneath the weld cavity (i.e., shoulder flow zone). It can furthermore be suggested that the weld cavity is the result of an insufficient supply of the shoulder zone material swirling downward from the retreating side to the advancing side, and needs to be fully filled with a sufficient amount of the shoulder zone material to form a defect-free weld. The weld cavity also provides a good geometric reference to the features of the shoulder zone produced by the scroll tool, which helps advance the existing weld zone formation theories summarized by Donatus et al. (Ref 14).

3.2 Shoulder Zone Origins and Characters

3.2.1 Features of Shoulder Zone. Figure 5(a) and (b) presents a 'marker-insert' post-weld profile and micrograph of the transverse cross section of the weld, obtained at a 0.5 mm depth of shoulder penetration with tool rotating while traveling at constant speeds 250 rpm and 40 mm/min. It can be observed



(a)



(b)

Fig. 5 Optical macrographs obtained from the weld made in 'marker-insert' experiment with 0.5 mm depth of shoulder penetration under tool rotating while traveling at constant speeds 250 rpm and 40 mm/min, (a) post-weld profile showing an embedded copper foil, and (b) transverse cross section of the weld showing a defect (void), copper foil insert on the AS, onion-rings and layer-to-layer structures in the upper and lower portion of the weld zone

from Fig. 5(b) that a defect (void) and copper foil insert presented on the weld transverse cross section. The presence of this small weld void suggests that the shoulder zone material flow was just slightly insufficient to fully fill the space left behind by the advancement of the tool pin. The void is in the advancing side of the weld zone, which is consistent with the weld cavity (i.e., larger void produced at 0.4 mm depth of shoulder penetration) illustrated in Fig. 4. In addition, a corn-shaped pattern with onion-rings structure in the upper portion and several layer-to-layer structures in the lower portion of the weld zone can be observed from Fig. 5(b), which is similar to the weld zone flow pattern shown in Fig. 3(b). According to previous studies (Ref 9, 17, 18), the onion-rings and layer-to-layer structures were formed due to the arc-shaped layers extruding and stacking behaviors by rotating tool, especially affected by the root portion of tool pin (Fig. 1).

3.2.2 Material Flow Movement in Shoulder Zone. Figure 6(a) presents an optical micrograph of the top portion of marker-insert weld's longitudinal cross section (sectioned through welding center line) with the marked areas of 'A' and 'B' for further investigation. It can be seen that there was a flow interface that potentially distinguished between the shoulder flow from nugget flow (measured band spacing $\lambda = 0.16$ mm). Furthermore, the thickness of proposed shoulder zone was 2.2 mm, which was nearly identical to the one (i.e., 2.0 mm) shown in Fig. 3(c), though these two welds were produced at two different depths of shoulder penetration (i.e., 0.5 mm vs

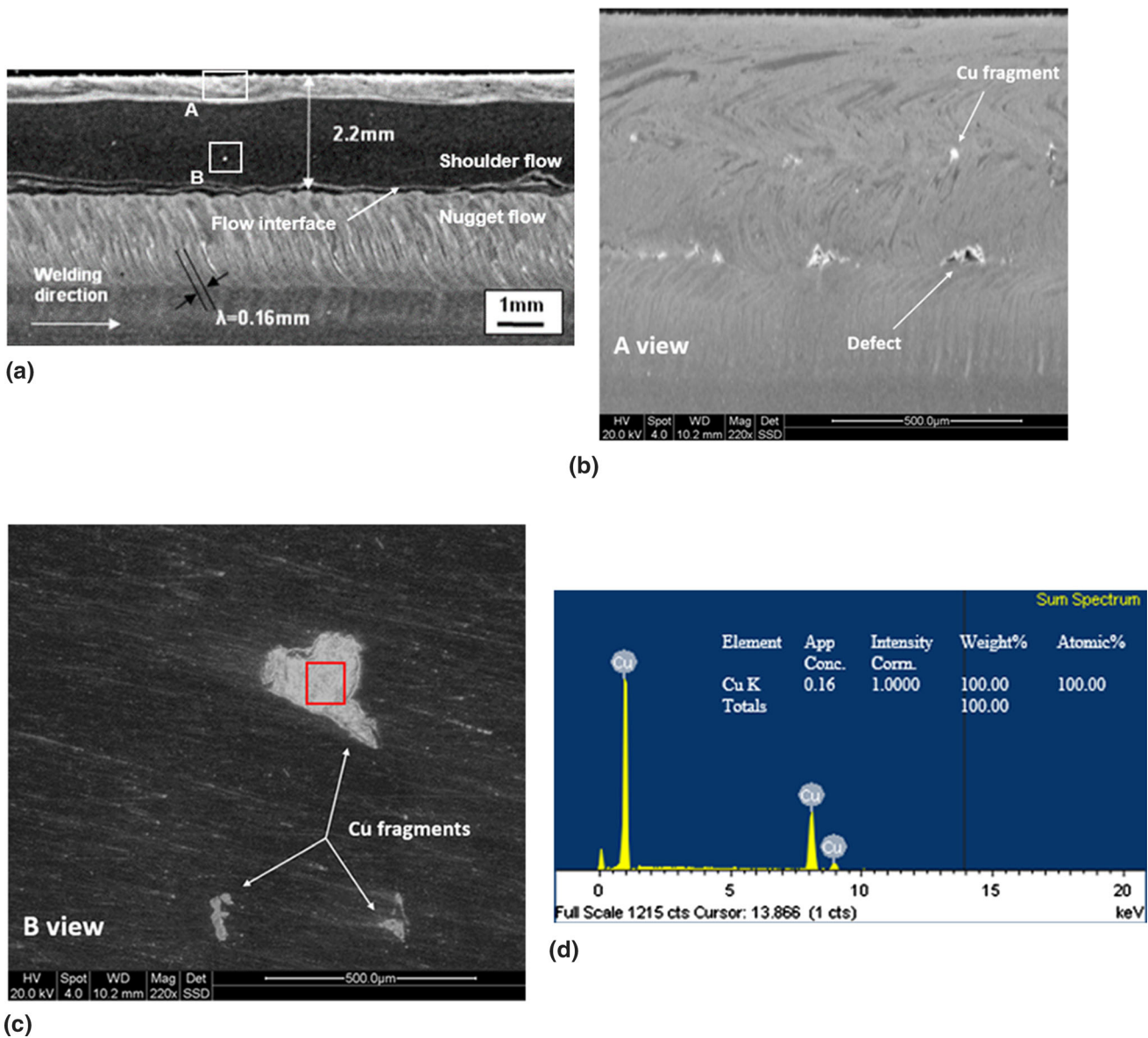


Fig. 6 Optical and SEM micrographs of the weld made in ‘marker-insert’ experiment at 0.5 mm depth of shoulder penetration, (a) macrograph of the top portion of weld longitudinal cross section indicating the material flow interface potentially distinguished between the shoulder flow and nugget flow and marked areas of ‘A’ and ‘B’, (b) SEM micrographs of area ‘A’ marked in (a) showing potential copper foil fragments (i.e., bright color particles) and an internal defect in the upper portion of shoulder zone, (c) SEM micrographs of area ‘B’ marked in (a) displaying potential copper foil fragments in the middle portion of shoulder zone and indicating a potential copper foil fragment framed by a red box for conducting EDS analysis, and (d) EDS spectra of the area in (c) framed by red box, showing chemical compositions of 100% Cu element

0.4 mm).

Figure 6(b) is a SEM micrograph of the area ‘A’ in the upper portion of the weld zone marked in Fig. 6(a), showing potential copper foil fragments, i.e., bright color particles (size around 35 μm) distributed within the weld zone. It can be observed that there was an internal defect in the weld zone, which correlated well with the defect presented in the weld transverse cross section shown in Fig. 5(b).

Figure 6(c) displays a SEM micrograph of the area ‘B’ marked in Fig. 6(a), presenting potential copper foil fragments distributed in the shoulder driven zone. It can be observed that these bright color particles were deformed and stretched to different sizes ranging from 71 to 335 μm , then finally

deposited in the middle portion of shoulder zone. The movement of these bright color particles (i.e., moving from upper portion to middle portion within the shoulder zone) supported the funding of Guerra et al. (Ref 19) that shoulder zone material moved along the vertical axis of the FS tool. To delineate the chemical compositions of these bright color particles, one largest particle (framed by a red box shown in the Fig.) was selected to conduct EDS analysis.

Figure 6(d) presents EDS spectra for the red box area framed in Fig. 6(c), and the EDS analysis (scanning the framed area) indicated that the bright color particle contains 100% Cu element. Indeed, the bright color particle is a Cu foil fragment, and this weld zone mixed with the Cu fragments is in fact the

shoulder driven zone. The confirmed deposition of Cu foil fragments in the shoulder zone strongly supported the hypothesized markers (i.e., Cu foil fragments) movement in this present study. Actually, the final deposited Cu foil fragments corresponded with the real depositing behavior of the shoulder driven zone material, providing a visible convenience to investigate the material flow movement in the shoulder zone. This outcome agreed with the results of Beygi et al. (Ref 20). And it also well correlated with the findings of Huang et al. (Ref 11) regarding the distribution of the copper foil markers in the ‘marker-insert’ weld, although they placed the Cu foils between the faying interface along the welding path, which was in a different configuration compared to this present study.

Accordingly, the shoulder driven zone can be located in the weld zone above the flow interface shown in Fig. 6(a). It is clear that firstly, after plunging the rotating scroll shoulder into the workpiece (i.e., 6061Al-T6 alloy in this present study), the workpiece material (including Al workpiece and Cu foil) was driven into the scroll groove beneath the tool shoulder to form the pick-up material (PUM). Then the PUM accumulated around the center of the scroll groove for forming the annular ring material (ARM). Lastly, when the tool was traveling forward simultaneously, the ARM was driven downward by the rotating threaded tool pin and deposited within the shoulder driven zone to form the FS weld structure.

3.2.3 Geometry Variation of Shoulder Zone. As suggested in the previous section (shown in Fig. 4), the thickness of the shoulder driven zone varied over the transverse direction of the weld zone. Figure 7(a), (b) and (c) shows optical micrographs of the top portion of marker-insert weld’s longi-

tudinal cross sections, obtained by sectioning the weld through the retreating side with 7.5 mm away from the welding center line, the welding center line, and the advancing side with 7.5 mm away from the welding center line, respectively. It can be noted that the shoulder driven zone has a thicker portion on the advancing side than the retreating side, and the shoulder zone thickness increased from 1.5 to 3.6 mm (measured along the weld transverse direction). This finding, for the first time provided actual experimental results to support the directed observation of the post-weld configuration shown in Fig. 4. Indeed, understanding of the weld zonal configuration variation is important as it helps improve FS tool design and optimize welding parameters to produce defect-free welds with the desired microstructure and properties. This finding is also in agreement with the findings of Donatus et al. (Ref 14) that material flow from the retreating side to the advancing side only occurs in the tool shoulder domain during scroll tool FSW, which implies that the material flows more into the advancing side from the retreating side in the shoulder driven zone.

3.3 Shoulder Zone Flow Patterns

Figure 8(a) and (b) displays a post-weld profile, and micrograph of the transverse cross section of weld, obtained at 0.6 mm depth of shoulder penetration with tool rotating while traveling at constant speeds of 250 rpm and 40 mm/min. It can be observed that no surface defect or internal voids appeared on the post-weld profile as well as micrograph of the weld transverse cross section. These observed weld features indicate that a sufficient amount of the shoulder zone material (generated under the current FS welding parameters) had been

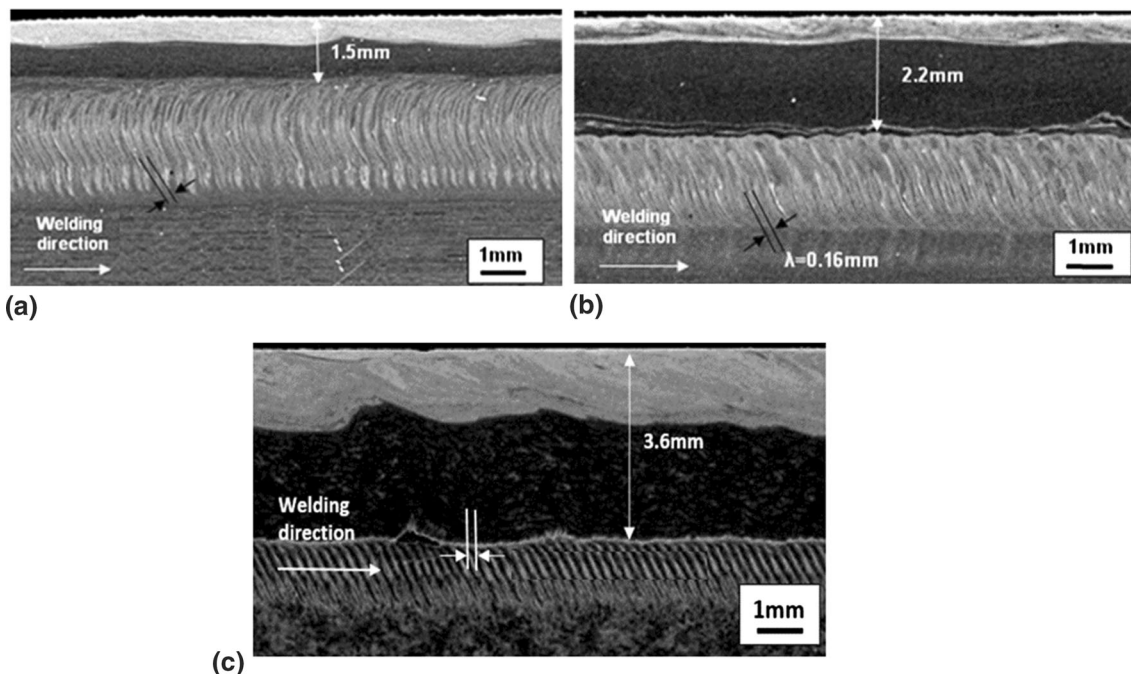


Fig. 7 Optical micrographs of the top portion of marker-insert weld’s longitudinal cross sections, obtained by sectioning the weld through: (a) retreating side with 7.5mm away from the welding center line, (b) welding center line, and (c) advancing side with 7.5mm away from the welding center line, indicating the increase of shoulder zone thickness from 1.5 to 3.6 mm measured along the weld transverse direction

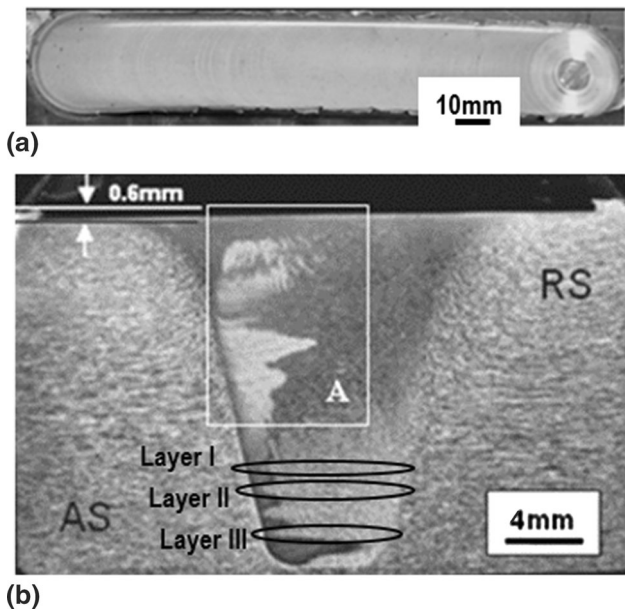
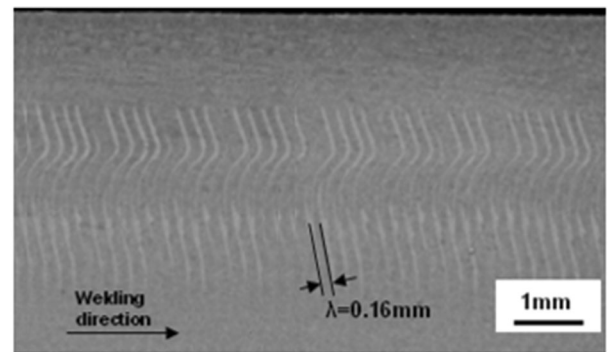


Fig. 8 Optical macrographs of the weld obtained at 0.6 mm depth of shoulder plunging with tool rotating while traveling at constant speeds of 250rpm and 40 mm/min, (a) post-weld profile showing no surface defect appeared, and (b) weld transverse cross section showing no internal defect (voids) occurred, appearance of several stacked layers, and marked area 'A' for high-magnification observation

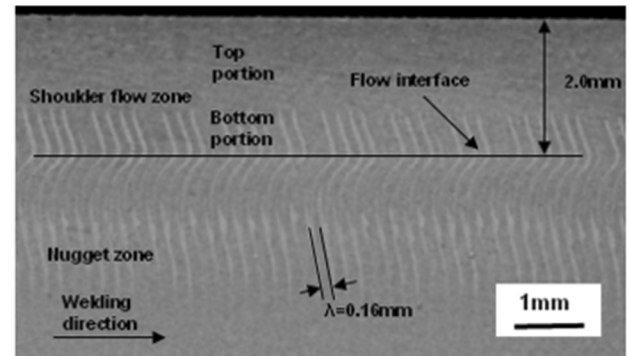
filled into the stable and forward moving cavity (shown in Fig. 4) left behind by the progression of the tool pin in full, and it thus led to the formation of this defect-free weld.

By examining Fig. 8(b), a clear corn-shaped pin zone flow pattern, including more than four stacked layers (e.g., layer I to III from up to bottom) and layer-to-layer structures of the area 'A', displayed in the weld zone, which was similar to those shown in Fig. 3(b) and 5(b). The forming mechanisms of the observed pin zone flow pattern can be suggested that during scroll tool FSW, the in-process material flow initially sticks inside the groove of threaded pin to rotate around the tool pin. While the tool pin is rotating, the pin threads trap the material flow to cause the flow's vertical movements, which results in several stacked layers appearing in the pin driven weld zone. The current experimentally obtained pin zone flow pattern well supports the numerical simulation of the pin zone flow behavior presented by Chen et al. (Ref 10). In addition, the current layer-to-layer structures (mainly distributed in the advancing side of the weld) show similar flow patterns compared to Donatus et al. (Ref 14) in dissimilar FSW of AA5083 and AA6082 alloys. They suggested that the layer-to-layer structures in the lower portion of the weld zone have a strong relation with the equivalent plastic strain field in the welds (Ref 14). The multiple layers or onion-rings structures stacked in the vertical direction of the weld zone have also been reported in (Ref 21, 22).

Figure 9(a) and (b) presents optical micrographs of two different-location longitudinal cross sections from the same weld obtained at 0.6 mm depth of shoulder penetration. It is clear that no internal defects occurred in these two different-location weld longitudinal cross sections. While carefully examining of Fig. 9(a), there are unique flow patterns, which show as serials of continuous large-scale vertical curves (less



(a)



(b)

Fig. 9 Optical micrographs of two different top portion of weld longitudinal cross sections from the same weld, obtained at 0.6 mm depth of shoulder plunging with tool rotating while traveling at constant speeds of 250 rpm and 40 mm/min, (a) showing serials of large-scale vertical curves measured horizontal spacing (λ) of 0.16 mm between two adjacent near parallel curves that appear repeatedly throughout the entire weld cross section, and (b) indicating flow interface between the shoulder flow zone and nugget zone, showing a simple layer-to-layer banded structure appeared in the bottom portion of shoulder flow zone, whereas featureless patterns remained in the top portion of the shoulder zone

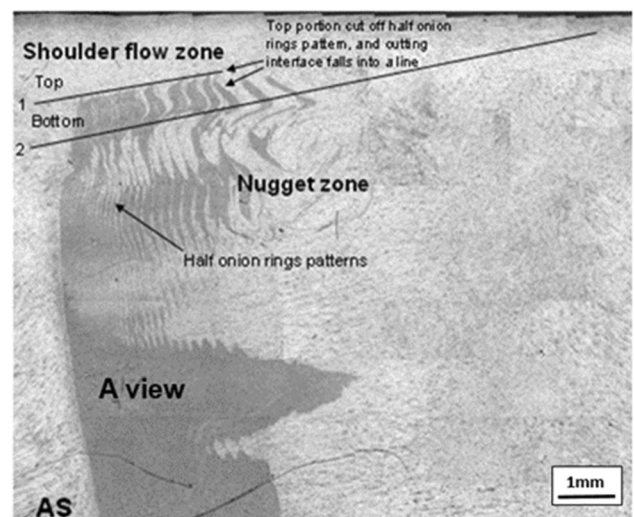


Fig. 10 Higher-magnification micrograph of the area 'A' marked in Fig. 8 (b) showing featureless patterns presented in the top portion of the shoulder flow zone, separated by line '1' from the bottom portion of the shoulder flow zone (which presents as a quarter of onion-rings patterns), and indicating a half of onion-rings patterns displaced in the nugget zone, separated from the shoulder flow zone by line '2'

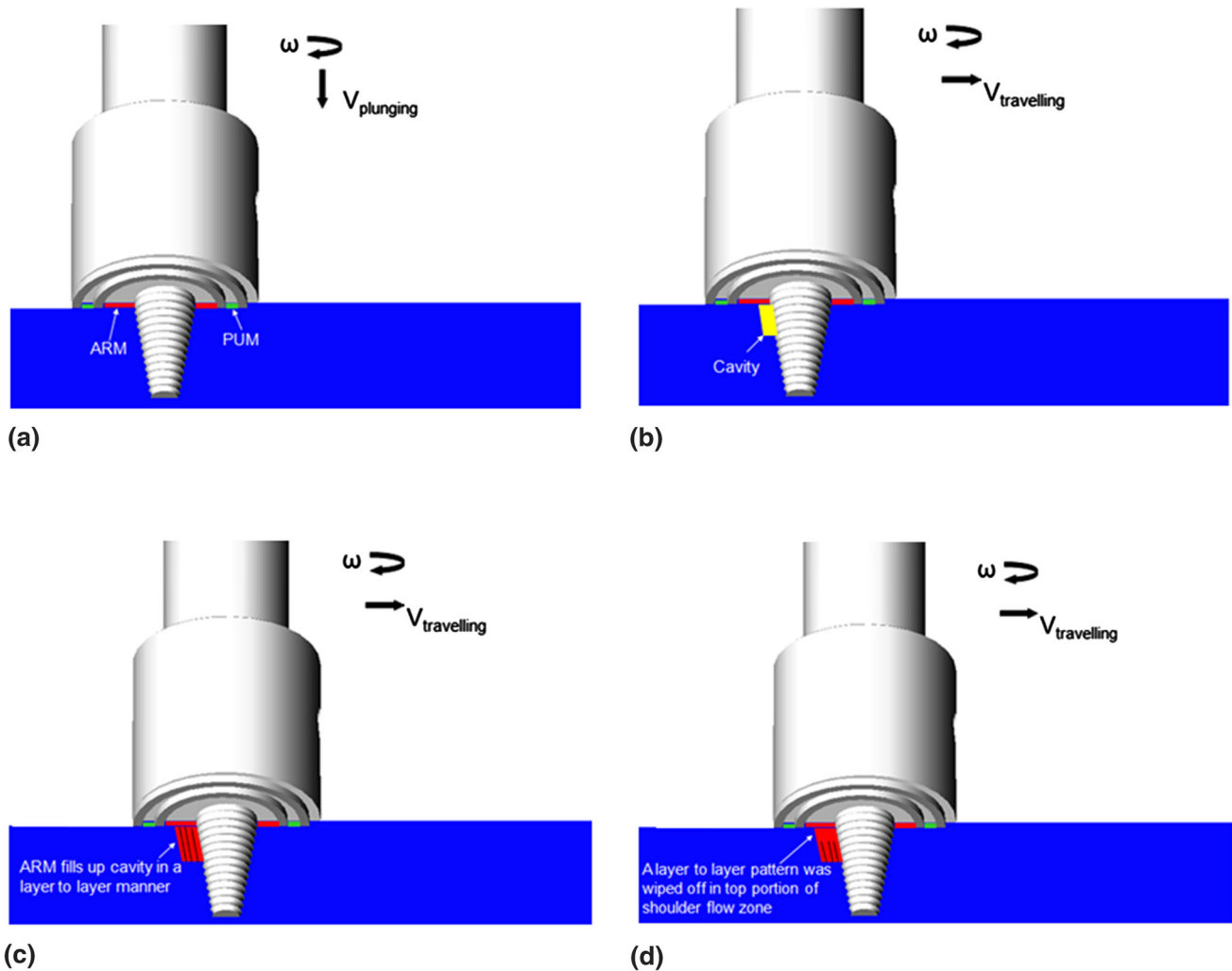


Fig. 11 Schematic 3D illustrations of scroll tool FSW process, (a) PUM and ARM formation, after plunging scroll tool into the workpiece at a certain depth, (b) a cavity formed, after tool moving forward, (c) filling up the cavity by ARM, simultaneously forming a shoulder flow zone with a layer-to-layer-manner, and (d) forming unique flow patterns in shoulder flow zone: the top portion of the layer-to-layer flow patterns are wiped off to form the featureless flow pattern, whereas the bottom portion of the layer-to-layer flow patterns remain

clear in the weld mid-section) with measured horizontal spacing (λ) of 0.16 mm between two adjacent near parallel curves, and appear repeatedly throughout the entire weld longitudinal cross section.

To interpret the above flow patterns, it is important to locate these patterns within the weld zone, thus, the shoulder zone thickness was set to 2.0 mm to pinpoint these flow patterns, and this value was adopted based on the previous measurements shown in Fig. 3(c) and 6(a) for the welds produced under the similar welding conditions. Accordingly, a horizontal solid line positioned at 2.0 mm below and parallel to the weld top surface was drawn onto Fig. 9(b), and this line acted as a flow interface to distinguish between the shoulder flow and nugget flow. After locating these flow patterns (i.e., serials of continuous large-scale vertical curves), it can be noted from Fig. 9 (b) that a simple layer-to-layer banded structure appeared in the bottom portion of the shoulder flow zone and nugget zone. Interestingly, these simple banded patterns were not presented in the top portion of the shoulder flow zone, instead of showing featureless patterns.

To cross-examine the flow patterns between the weld longitudinal and transverse cross sections, a higher-magnification micrograph of the area 'A' marked in Fig. 8(b) is presented in Fig. 10. In which the unique flow patterns including featureless patterns on the top and a quarter of onion-rings patterns (i.e., layer-to-layer structures) at the bottom, separated by line '1' had appeared in the top portion of the weld zone. Indeed, this top portion of the weld zone is shoulder driven zone, distinguished from the nugget zone by line '2'. And after verifying the flow patterns shown in Fig.10 and 9(b), it can be found that the shoulder zone flow pattern presented in the weld transverse cross section is in accordance well with the flow patterns shown in the weld longitudinal cross section.

Furthermore, these two distinct flow features (Fig. 10) seem to be constructed in such a way that the top portion of a half of onion-rings patterns are cut off to form the featureless patterns (due to the flow interactions) on the top of the weld zone. While the bottom portion of the half of onion-rings patterns are retained presenting as a quarter of onion-rings patterns at the bottom of the weld zone. This finding explains the forming mechanisms of the

layer-to-layer structures in the shoulder zone, which advances the existing shoulder zone theories reported in (Ref 23, 19, 24).

3.4 Shoulder Zone Forming Mechanism

Based on the verified flow patterns shown in Fig. 9(b) and 10, the forming mechanism of shoulder flow zone is proposed as follows. When the scroll tool is plunged into the workpiece to certain depth (Fig. 11a), the workpiece material is plasticized by the tool, and pushed up into the scroll groove beneath the tool shoulder forming the pick-up materials (PUM). The PUM accumulates around the root portion of the pin, and the central portion of the PUM forms annular ring material (ARM).

While the tool is moving forward, as indicated in Fig. 11(b), a cavity (real features shown in Fig. 4) is formed as a result of the nugget zone material (i.e., shear layers) being driven downward by the screwing action of the tool pin, and detached from the trailing-retreating location. Simultaneously, the ARM is pushed by the incoming PUM resulted from the tool forward movement, and driven downward by the root portion of the threaded pin, and then detached at the trailing-retreating location of the tool pin to fill up the cavity. The interactions between the forming of the cavity beneath the ARM and simultaneously filling up the cavity by the ARM detachments form the shoulder flow zone in a layer-to-layer manner (Fig. 11c).

As FSW continues, the top portion of the detached layered-ARM is interrupted by the wiping motion of the bottom face of the remaining ARM beneath the tool shoulder. This interruption leads to the formation of a distinct top portion of the shoulder flow zone without a layer-to-layer attribute. Whereas the bottom portion of the shoulder flow zone still remains a layer-to-layer manner (Fig. 11d).

4. Conclusions

The present study analyzes the weld configuration, characters and flow patterns of shoulder driven zone during scroll tool FSW. A series of FSW of thick section 6061 Al-T6 and Cu-AstmB370 foil trials was conducted, and the produced welds were characterized via OM, SEM and EDS to reveal the weld zone characters including zonal flow patterns. For the first time, the Cu foil as tracer was placed outside the welding path to visualize the shoulder flow zone material movement so as to identify the shoulder zone and zonal flow patterns. Based on the results obtained from this present study, the following conclusions can be drawn:

1. A special corn-shaped pattern can be found in the weld stir zone presenting with several stacked layers from up to bottom, which corresponds to the tapered pin tool used in this present FSW experiments.
2. The thickness of shoulder driven zone was measured around 2.0 to 2.2 mm. It varies along the weld transverse cross section with a thicker portion on the advancing side than the retreating side.
3. The location of actual shoulder driven zone was pinpointed based on the distribution of the copper foil fragments (size ranges from 35 to 335 μm) within the weld zone.
4. The verified shoulder zone flow patterns consist of a simple layer-to-layer banded structure appearing in the bottom portion of the shoulder driven zone, whereas a featureless flow pattern showed in the top portion of the shoulder zone.

5. The shoulder zone forming mechanism is suggested as follows. When the tool pin and shoulder are plunged into the workpiece to a certain depth, the workpiece material is extruded by the tool and pushed up into the scroll groove beneath the tool shoulder forming the pick-up material. Then the central portion of the pick-up material is driven downward by the root portion of the tool pin and detaches from the tip portion of the pin in a layer-to-layer manner forming the shoulder driven zone.

Acknowledgment

The authors acknowledge the support of this study by the University Faculty RSCA Awards, San Jose State University.

Reference

1. N. Dialami, M. Cervera and M. Chiumenti, Defect formation and material flow in Friction Stir Welding, *Eur. J. Mech. A Sol.*, 2020, **80**, p 103912.
2. N. Gotawala and A. Shrivastava, Analysis of material distribution in dissimilar friction stir welded joints of Al 1050 and copper, *J. Manuf. Process.*, 2020, **57**, p 725–736.
3. W.J. Arbegast, A flow-partitioned deformation zone model for defect formation during friction stir welding, *Scripta Mater.*, 2008, **58**(5), p 372–376.
4. T.K. Bhattacharya, H. Das and T.K. Pal, Influence of welding parameters on material flow, mechanical property and intermetallic characterization of friction stir welded AA6063 to HCP copper dissimilar butt joint without offset, *Trans. Nonferr. Metals Soc. China*, 2015, **25**(9), p 2833–2846.
5. W.F. Xu, J.H. Liu and D.L. Chen, Material flow and core/multi-shell structures in a friction stir welded aluminum alloy with embedded copper markers, *J. Alloy. Compd.*, 2011, **509**(33), p 8449–8454.
6. L.H. Ahmad Shah et al., Influence of tool eccentricity on the material flow and microstructural properties of AA6061 aluminum alloy friction stir welds, *J. Alloys Compd.*, 2020, **826**, p 154219.
7. K.K. Mugada and K. Adepur, Effect of knurling shoulder design with polygonal pins on material flow and mechanical properties during friction stir welding of Al–Mg–Si alloy, *Trans. Nonferr. Metals Soc. China*, 2019, **29**(11), p 2281–2289.
8. R.S. Mishra and Z.Y. Ma, Friction stir welding and processing, *Mater. Sci. Eng. R. Rep.*, 2005, **50**(1–2), p 1–78.
9. K. Kumar and S.V. Kailas, The role of friction stir welding tool on material flow and weld formation, *Mater. Sci. Eng., A*, 2008, **485**(1), p 367–374.
10. G. Chen et al., Effects of pin thread on the in-process material flow behavior during friction stir welding: a computational fluid dynamics study, *Int. J. Mach. Tools Manuf.*, 2018, **124**, p 12–21.
11. Y. Huang et al., Material-flow behavior during friction-stir welding of 6082–T6 aluminum alloy, *Int. J. Adv. Manuf. Technol.*, 2016, **87**, p 1–9.
12. Z.W. Chen, T. Pasang and Y. Qi, Shear flow and formation of Nugget zone during friction stir welding of aluminium alloy 5083-O, *Mater. Sci. Eng., A*, 2008, **474**(1–2), p 312–316.
13. R. Rai et al., Review: friction stir welding tools, *Sci. Technol. Weld. Joining*, 2011, **16**(4), p 325–342.
14. U. Donatus et al., Flow patterns in friction stir welds of AA5083 and AA6082 alloys, *Mater. Des.*, 2015, **83**, p 203–213.
15. Y. Tozaki, Y. Uematsu and K. Tokaji, Welding structure and tensile-shear properties of friction-stir spot welds joined by scrolled groove shoulder tool without probe in aluminium alloy, *Nihon Kikai Gakkai Ronbunshu A Hen/Trans. Jpn. Soc. Mech. Eng. Part A*, 2009, **75**(750), p 228–234.
16. K.N. Krishnan, On the formation of onion rings in friction stir welds, *Mater. Sci. Eng., A*, 2002, **327**(2), p 246–251.
17. K. Colligan, Material flow behavior during friction stir welding of aluminum, *Weld. J.*, 1999, **78**, p 229–237.

18. Imaizumi, T., et al., *Three-dimensional visualization of material flow during friction stir welding for steel and aluminum by two pairs of X-ray transmission systems*, in *Proceedings of the 1st International Joint Symposium on Joining and Welding*. 2013, Woodhead Publishing. p. 359-361
19. M. Guerra et al., Flow patterns during friction stir welding, *Mater. Charact.*, 2002, **49**(2), p 95–101.
20. R. Beygi et al., Influence of tool geometry on material flow and mechanical properties of friction stir welded Al-Cu bimetals, *J. Mater. Process. Technol.*, 2018, **255**, p 739–748.
21. Z.W. Chen and S. Cui, On the forming mechanism of banded structures in aluminium alloy friction stir welds, *Scripta Mater.*, 2008, **58**(5), p 417–420.
22. A. Tongne et al., On material flow in Friction Stir Welded Al alloys, *J. Mater. Process. Technol.*, 2017, **239**, p 284–296.
23. R.M. Leal et al., Material flow in heterogeneous friction stir welding of thin aluminium sheets: effect of shoulder geometry, *Mater. Sci. Eng., A*, 2008, **498**(1–2), p 384–391.
24. C.-S. Wu et al., Visualization and simulation of plastic material flow in friction stir welding of 2024 aluminium alloy plates, *Trans. Nonferr. Metals Soc. China*, 2012, **22**(6), p 1445–1451.

Publisher's Note Springer Nature remains neutral with regard to jurisdictional claims in published maps and institutional affiliations.